Paper 6-3 has been designated as a Distinguished Paper at Display Week 2018. The full-length version of this paper appears in a Special Section of the *Journal of the Society for Information Display (JSID)* devoted to Display Week 2018 Distinguished Papers. This Special Section will be freely accessible until December 31, 2018 via:

http://onlinelibrary.wiley.com/page/journal/19383657/homepage/display_week_2018.htm

Authors that wish to refer to this work are advised to cite the full-length version by referring to its DOI:

https://doi.org/10.1002/jsid.637

Highly Efficient Fluorescent Blue Materials and Their Applications for Top Emission OLEDs

Tetsuya Masuda, Yuki Nakano, Yoshiaki Takahashi, Hirokatsu Ito, Keiji Okinaka, Emiko Kambe, Yuichiro Kawamura and Hitoshi Kuma

Idemitsu Kosan Co., Ltd., Chiba, Japan

Abstract

We developed new fluorescent blue dopants (BDs) for achieving high efficient blue organic light emitting diode (OLED). The new BD showed both high photoluminescent quantum yield >0.9 and highly horizontal orientation (S'>0.9) in the doped film with keeping a chemical stability by introducing suitable substituents. We developed hole transporting materials and optimized the combination of hole transporting layers to decrease a carrier accumulation at the interface between electron blocking layer/emission layer (EML). We found that the external quantum efficiency dependency from low to high current density was turned flat by promoting hole injection into EML. The Top-Emission OLED using the new BD and the optimized device architecture exhibited high efficiency of L/J/CIEy around 200 at CIEy=0.043.

Author Keywords

Orgainc light emitting diode, Blue dopant, Molecular orientation, Fluorescence, Photoluminescence, Impedance spectroscopy, Top-Emission

1. Introduction

Recently, Organic light emitting diode (OLED) is becoming rapidly spread as the corner of the high-end products such as a large-sized 4K HDR TV and a full-screen smart phone [1]. Meanwhile, further improvement is required for reduction of power consumption, durability against burn-in, and color change suppression due to viewing angle in the future. Very recently, new mechanisms such as thermally activated delayed fluorescence have attracted attentions [2], but the development of materials that cover the required performances for display (efficiency, lifetime and color purity in each of RGB) are still on the way. Regarding efficiency in fluorescent OLED, as we have discussed about the theoretical limit of four elements that control the external quantum efficiency of OLEDs [3][4][5], it is necessary to improve photoluminescent quantum yield (PLQY) of light emitting material itself, light extraction, and Triplet-Triplet Fusion (TTF) efficiency [6], respectively.

OLED has a high potential to describe a true black, but the improvement of RGB balance in the low brightness is needed to get high quality gray scale, especially in the side-by-side RGB devices. We tried to improve the efficiency of blue at low current density since fluorescent blue and phosphorescent red and green have a different dependency of efficiency vs current density.

In this paper, as solutions to the issues shown above, we report (1) improvement of EML, especially development of new BDs and (2) improvement of device architectures (optimization of materials and combinations, charge balance, optical cavity length, reflective electrode).

2. Results and discussions

2-1. High Efficient Fluorescent Blue Dopants:

In general, the external quantum efficiency (η_{ext}) of an OLED is described by the following four factors as,

$$\eta_{ext} = \gamma \times \eta_r \times \eta_{PL} \times \eta_{OC} \quad (1)$$

where recombination probability is γ, exciton generation ratio is η_r, PLQY is η_{PL}, and light out-coupling efficiency is η_{OC}.

Now γ value is assumed to be 100% and η_r could be assumed to be 40% by utilizing TTF ideally in case of fluorescent device. On the other hand, regarding η_{PL} and η_{OC}, η_{PL} depends on the value of corresponding BD in a doped film and it is known that η_{OC} also strongly depends on molecular orientation horizontally induced by the structure of BD [3]. It means that BD design can increase η_{PL} and improve its orientation in a film. We examined several structures for BD in order to realize high η_{PL} and horizontal orientation in the desired wavelength range.

(a) Improvement of PLQY

In order to improve η_{PL} of molecule, generally, it is important to increase the oscillator strength and improve the emission rate constant, and it is effective to increase the rigidity for suppressing deactivation by vibrational relaxations.

Figure 1 shows relationship of the emission peak wavelength and η_{PL} for various BDs in toluene. Although the η_{PL} of the conventional BD group were around 0.85, it was confirmed that the structure newly introduced achieved higher η_{PL} over 0.9. The emission peak and η_{PL} of the conventional BD-1 (filled blue diamond) and the new BD-2 (filled red circle) were 449, 452 nm, and 0.84, 0.92, respectively.

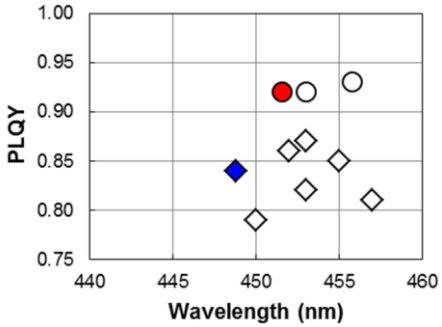

Figure 1. Emission wavelength vs PLQY on various blue dopants in toluene. Conventional and new structures were plotted by diamond and circle, respectively.

 ISSN 0097-996X/18/4701-0052-$1.00 © 2018 SID

Table 1. Photophysical properties of BD-1 and BD-2.

PLQY and transient PL decay were measured in the doped film.

	η_{PL}	$\tau_{obs.}$ [s]	k_r [s^{-1}]	k_{nr} [s^{-1}]
BD-1	0.81	2.7×10^{-9}	3.0×10^{8}	7.0×10^{7}
BD-2	0.91	3.0×10^{-9}	3.0×10^{8}	3.0×10^{7}

Table 1 shows η_{PL} and transient PL lifetime ($\tau_{obs.}$) of BD-1 and BD-2 in the doped film into blue host (BH-1). Here η_{PL} and $\tau_{obs.}$ can be described by radiative rate constant (k_r) and non-radiative decay rate constant (k_{nr}) as follows,

$$\eta_{PL} = k_r / (k_r + k_{nr}) \quad (2)$$

$$\tau_{obs.} = 1 / (k_r + k_{nr}) \quad (3)$$

$$k_r = \eta_{PL} / \tau_{obs.} \quad (4)$$

The calculated values of k_r and k_{nr} are also shown in Table1. Since there is no difference between k_r of BD-1 and BD-2, the η_{PL} improvement in BD-2 should be suggested that non-radiative deactivation is suppressed.

(b) Molecular orientation

The molecular orientation of each BD in the film is shown in Figure 2. The orientation factor (S') was calculated from the spectroscopic ellipsometry of the neat film [7]. It was found that BD-2 could realize both high ηPL >0.9 and high S' value >0.9. Furthermore, we checked the results in the films that BDs were doped into BH-1 (Figure 2, upper). From the results of angular dependency of PL intensity measurement [8], it was confirmed that the series of BDs retained the same orientation characteristics as the neat film even in the host (Figure 2, bottom). This is a result that efficiency improvement can be expected in a practical device.

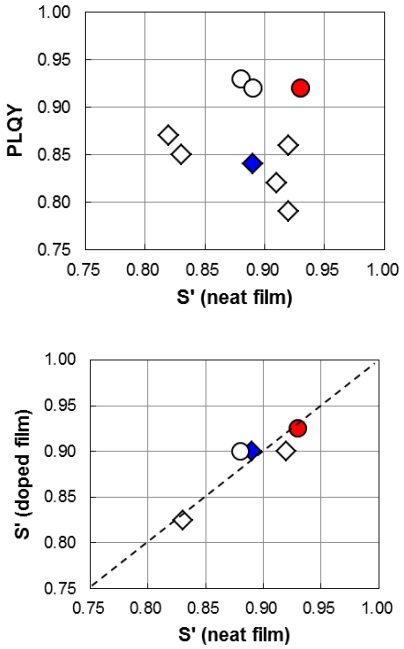

Figure 2. [upper] PLQY in toluene solution vs Orientation Factor (S') on various blue dopants. [bottom] Orientation Factor (S') in neat film vs in doped film.

(c) Bottom emission device performances

Bottom emission (BE) OLEDs using BD-1 and BD-2 were fabricated. The device structure is as follows. The results are shown in Table 2 and Figure 3. In comparison BD-1 with BD-2, η_{ext} of BD-2 device was improved from 9.7% to 10.7% at 10mA/cm^2, corresponding to improvement of η_{PL} and S'.

Device-A :

ITO(130) / HI(10) / HT-1(80) / EB-1(10) / BH-1:BD(25:4%) / HB-1(5) / ET-1(20) / LiF(1) / Al(80) (nm)

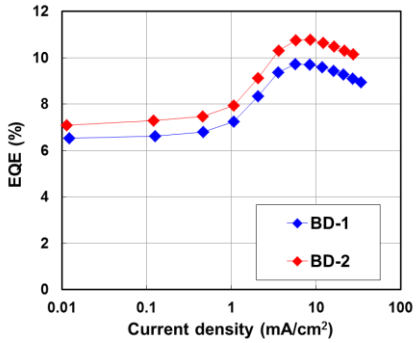

Figure 3. EQE dependency as a function of current density in Device-A with **BD-1 (blue)** and **BD-2 (red)**.

Table 2. Device performances of bottom-emission devices using BD-1 and BD-2 at the current density of 10 mA/cm^2.

	Voltage [V]	CIE		L/J [cd/A]	η [lm/W]	η_{ext} [%]	λ_p [nm]
		x	y				
BD-1	3.4	0.138	0.091	8.0	7.3	9.7	455
BD-2	3.4	0.136	0.100	9.5	8.6	10.7	458

2-2. Approaches for Improvement of Device Efficiency:

(a) BE device and Transient EL with HT-2 and EB-2

As we mentioned in the opening sentence, the improvement of RGB balance in the low brightness is needed to get high quality gray scale, especially in the side-by-side RGB devices. We need to try improvement of blue fluorescence efficiency at low brightness region. We fabricated two bottom emission devices using the material combination of HT-1 and EB-1 (Device-A) and HT-2 and EB-2 (Device-B). The device structures are as follows.

Device-A :

ITO(130) / HI(10) / **HT-1(80)** / **EB-1(10)** / BH-1:BD-2(25:4%) / HB-1(5) / ET-1(20) / LiF(1) / Al(80) (nm)

Device-B :

ITO(130) / HI(10) / **HT-2(80)** / **EB-2(10)** / BH-1:BD-2(25:4%) / HB-1(5) / ET-1(20) / LiF(1) / Al(80) (nm)

The results are shown in Table 3 and Figure 4. Efficiency at low current density region is improved by using HT-2 and EB-2 with good hole injection.

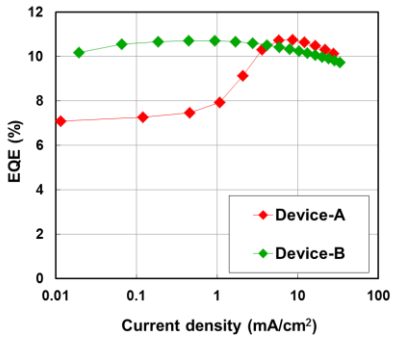

Figure 4. EQE dependency as a function of current density in **Device-A (red)** and **Device-B (green)**.

Table 3. Device performances of Bottom-emission devices using Device-A and Device-B at the current density of 10 mA/cm^2.

Device	Voltage [V]	CIE		L/J [cd/A]	η [lm/W]	η_{ext} [%]	λ_p [nm]
		x	y				
A	3.4	0.136	0.100	9.5	8.6	10.7	458
B	3.8	0.136	0.099	9.0	7.3	10.3	457

In order to investigate the factor of the efficiency improvement at low current density region, we checked the Triplet-Triplet Fusion (TTF) ratio by measurement transient EL. Transient EL responses were monitored by a photomultiplier tube (Hamamatsu Photonics K.K. R928). The photocurrents were entered directly into an input channel of a digital oscilloscope (Tektronix, Inc 2440) with an impedance of 50 Ω. The devices were connected serially to a pulse generator (Agilent Technologies, Inc. 8114A) and another channel of the oscilloscope with the impedance of 50 Ω. The repetition rate was 20 Hz and the pulse width was 500 μs. The signals of photocurrent were averaged on the oscilloscope till the signals became sufficiently smooth and then they transferred to a PC. Measurement of transient EL makes it possible to separate EL emission into the prompt emission component and the delay emission component. The delayed fluorescent component should be derived from TTF. In this paper, we refer to the delayed fluorescent component as TTF ratio. The results of transient EL are shown in Figure 5. Compared Figure 4 with Figure 5, it can be seen that current density dependence of EQE is consistent with that of TTF ratio. Therefore, low efficiency of Device-A at low current density region is attributed to be caused by quench of TTF components.

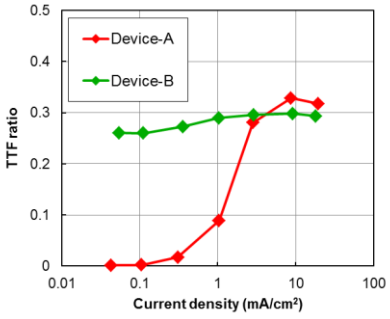

Figure 5. TTF ratio dependency as a function of current density in **Device-A (red)** and **Device-B (green)**.

(b) Carrier accumulations in hole only device

The maximization of the TTF efficiency should be required to maximize the efficiency of fluorescent OLEDs. We have previously reported that adjusting the charge balance in the EML could lead to suppress the triplet quenching by excess electrons and to improve the TTF efficiency [9]. In the Device-B, we assumed that the improvement of efficiency at low current density was due to the elimination of excess electrons by efficient hole injection into EML. To investigate this hypothesis, Hole only devices (HODs) with various HT combination were prepared and the presence of hole accumulation at each interface was examined from the shape of the arcs in the Cole-Cole plots on the measurement of Impedance spectroscopy (IS).

IS measurements were carried out using a Solartron 1260 impedance analyzer with a 1296 dielectric interface in the frequency sweep range from 100 mHz to 1MHz at room temperature. The AC oscillation amplitude was 100 mV.

In the device which has stacked organic layers, each layer is expressed as a parallel circuit of capacitor and resistance. At this time, the equation of complex impedance (Z) is described as follow,

$$Z(\omega) = \frac{R}{1 + j\omega RC} \tag{5}$$

Here, ω is angular frequency, R is resistance, and C is capacitance. The plot of real part and imaginary part of Z(ω) is called Cole-Cole plots. In case single layer of organic material, Cole-Cole plot becomes one arc. The modulus (M) is defined as follow,

$$M(\omega) \equiv j\omega Z = \frac{1}{C}\left(1 - \frac{1}{1 + j\omega RC}\right) \tag{6}$$

The arc also appears in the Cole-Cole plot of M(ω) as with the arc in that of Z(ω). From the equation 6, the diameter of the arc in Cole-Cole plot of M(ω) is 1/C. The thickness (d) of the condenser is described as following equation,

$$d = \varepsilon \frac{S}{C} \tag{7}$$

Here, ε is relative dielectric constant, and S is area. Considering that the relative dielectric constant of the organic material is about 3, the real part in the Cole-Cole of M(ω) can be converted to the film thickness of organic layers. It is possible to visualize the difference in conductivity of each layer by plotting the film thickness on the horizontal axis and M(ω) on the vertical axis. The presence of hole accumulation at each interface was examined from the shape of the arcs in the Cole-Cole plots by fabricated HODs, and we examined the relationship between hole accumulation and efficiency in low current density region. HOD structures for IS are shown as follow,

HOD-A :

ITO(130) / HI(10) / **HT-1(80)** / **EB-1(10)** / BH-1:BD-2(25:4%) / Al(80) (nm)

HOD-B :

ITO(130) / HI(10) / **HT-2(80)** / **EB-2(10)** / BH-1:BD-2(25:4%) / Al(80) (nm)

As shown in Figure 6, HOD-A and HOD-B that were corresponding to the Device-A and Device-B showed different peaks in the cole-cole plots by changing the combination of HTL and EBL. In the HOD-A, the multiple peaks were observed from the low current density region and they were attributed to the accumulation of holes at the EBL/EML interface. On the other hand, HOD-B showed no clear multiple peaks in the whole voltage range, suggesting that there was no hole accumulation at the interface.

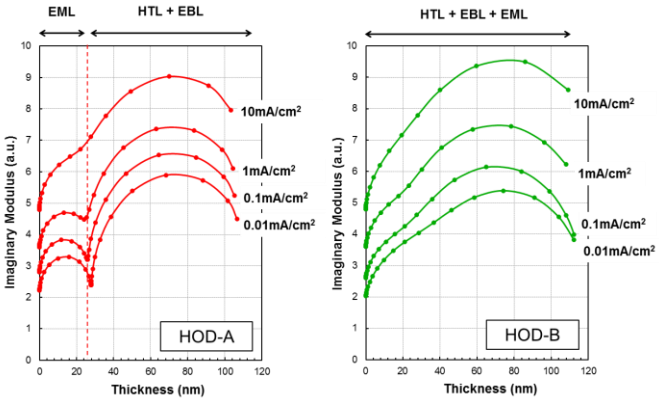

Figure 6. Cole-Cole plots of HOD structures measured by Impedance Spectroscopy.

2-3. Top Emission Device Properties:

Finally, the top emission device was fabricated by combining BD-2, and optimized materials as Device-C. The optical cavity length was adjusted by the thickness of organic layers. In the top emission device, anode reflectance also greatly affects the efficiency. We used the high reflective substrate of Ag-alloy/ITO (hereinafter Ag/ITO) [10]. The Device-C structure is as follows.

Device-C :

Ag/ITO(10) / HI(10) / HT-2(113) / EB-1(5) / BH-1:BD-2(20:2%) / HB-1(5) / ET-1(20) / LiF(1) / Mg:Ag(12:90%) / Cap(65) (nm)

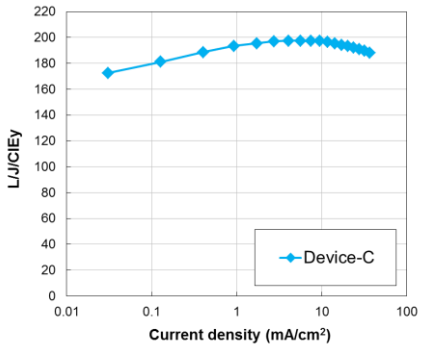

Figure 7. L/J/CIEy dependency as a function of current density.

As a result, the Device-C shows L/J/CIEy of 197 at CIEy=0.043 and it showed LT95@10mA/cm^2 of 650 hours. Maximum L/J/CIEy reached at 200 and a flat L/J/CIEy curve was achieved with keeping over L/J/CIEy of 170 in the whole current density range.

Table 4. Device performances of Device-C at the current density of 10 mA/cm^2.

Voltage [V]	CIE		L/J [cd/A]	η [lm/W]	L/J/CIEy	λ_p [nm]	LT95 [h]
	x	y					
3.8	0.142	0.043	8.4	6.9	197	458	650

3. Summary

The efficiency of the organic EL device could be improved by developing highly efficient and horizontally oriented BD. The presence of hole accumulation at each interface was examined from the shape of the arcs in the Cole-Cole plots, and we examined the relationship between hole accumulation and efficiency in low current density region. As a result, efficiency of the device with less hole accumulation was improved in the low current density region. We fabricated top emission device with optimized material combination, device structure and substrate reflectance. It shows L/J/CIEy of 197 at CIEy=0.043 and LT95 of 650 hours at the current density of 10mA/cm^2.

4. Acknowledgements

We thank Mitsubishi Materials Corporation for supplying Ag/ITO substrate which is used Ag sputtering target “Ag alloy No.201”.

5. References

[1] H. J. Noh, et al., 2017 INTERNATIONAL SYMPOSIUM DIGEST OF TECHNICAL PAPERS, p.1038 (2017)

[2] H. Nakanotani, et al., “High-efficiency organic light-emitting diodes with fluorescent emitters“, Nature Communications, 5, 4016 (2014)

[3] M. Kawamura, et al., 2010 INTERNATIONAL SYMPOSIUM DIGEST OF TECHNICAL PAPERS, p.560 (2010)

[4] Y. Kawamura, et al., 2011 INTERNATIONAL SYMPOSIUM DIGEST OF TECHNICAL PAPERS, p. 829 (2011)

[5] H. Kuma and C. Hosokawa, “Blue fluorescent OLED materials and their application for high-performance devices”, Science and Technology of Advanced Materials, 15, 034201 (2014)

[6] D. Y. Kondakov, et al., “Characterization of triplet-triplet annihilation in organic light-emitting diodes based on anthracene derivatives”, Journal of Applied Physics 102, 114504 (2007)

[7] T. Ogiwara et al., “Efficiency improvement of fluorescent blue device by molecular orientation of blue dopant”, Journal of the Society for Information Display, 22, 76–82, (2014)

[8] J. Frischeisen, et al., “Determination of molecular dipole orientation in doped fluorescent organic thin films by photoluminescence measurements“, Appl. Phys. Lett. 96, 073302 (2010)

[9] K. Okinaka, et al., 2015 INTERNATIONAL SYMPOSIUM DIGEST OF TECHNICAL PAPERS, p.312 (2015)

[10] Y. Hayashi et al., “The Atmosphere Dependence of Annealing for Anode”, IDW’17 OLED3-3 (2017)